On the nature of meander instability

Stefano Lanzoni[1] and Giovanni Seminara[2]

Received 28 September 2005; revised 31 May 2006; accepted 28 June 2006; published 4 November 2006.

[1] Bend instability is the process whereby perturbations of the planform distribution of a channel relative to a straight configuration may grow, driven by erosion at concave banks and deposition at convex banks, leading to the development of a meandering pattern. Here we investigate the nature of this instability; that is, we ascertain under what conditions bend instability is convective or absolute. In the former case, an initial nonpersistent, small perturbation localized in space is convected away, eventually leaving the flow domain unperturbed. In the latter case, perturbations spread in both the upstream and downstream directions, eventually affecting the whole flow domain. In convective instabilities, the spatial-temporal development of perturbations is somewhat dependent on the characteristics of the initial perturbation which is required to be persistent in time. On the contrary, absolute instabilities are able to amplify perturbations, even if triggered at some initial time and then ceased. If bend instability is convective, planform information migrates only in one direction, while in the absolute regime, information is propagated in both directions. We show that bend instability is most often, though not invariably, convective at both a linear and nonlinear level. Moreover, the group velocity of perturbations changes sign as the width to depth ratio of the channel crosses some threshold value (the resonant value of Blondeaux and Seminara (1985)): Below (above) resonance, information is propagated downstream (upstream). We discuss the implications that these findings have on the morphological characteristics of meandering rivers (in particular, the sense of skewing of meander bends and the direction of meander migration). We also clarify how the choice of appropriate boundary conditions in numerical simulations of planform evolution is crucially dependent on the nature of bend instability and on its subresonant or superresonant regime.

Citation: Lanzoni, S., and G. Seminara (2006), On the nature of meander instability, *J. Geophys. Res.*, *111*, F04006, doi:10.1029/2005JF000416.

1. Introduction

[2] River meandering provides an example of a striking regular pattern, ubiquitous in nature, which has long attracted the interest of scientists [e.g., *Einstein*, 1926]. Meandering develops in virtually all sedimentary environments, including gravel and sandy rivers (Figures 1a and 1b), incised rocky environments (Figure 1c), tidal channels, and salt marshes (Figures 1d and 1e). Gigantic meandering channels are shaped by turbidity currents in submarine fans at the base of the continental slope [*Imran et al.*, 1999]. Inactive meandering channels have also been detected in some of the pictures of the Mars surface collected by Viking and, more recently, within the framework of the Mars Orbiter Laser Altimetry project [*Moore et al.*, 2003; *Mazzocco*, 2005].

[3] River meandering belongs to a class of sedimentary processes occurring at the spatial scale of channel width, whose expression is the well known formation of large-scale bed forms called bars. The literature on the related phenomena of bar formation and meander development is vast and several observed features have been at least qualitatively understood through the wide and fruitful involvement of various research groups. The reader interested in the state of the art on the subject is referred to *Ikeda and Parker* [1989]. Later developments have been reviewed by *Repetto et al.* [1999] and, most recently, by *Seminara* [2005].

[4] Here, we focus on a fundamental issue concerning meander development which, to our knowledge, is so far insufficiently understood. What is the role of boundary conditions on the planform evolution of meandering rivers? In particular, can evolution be determined by constraints imposed in the downstream reach; that is, can upstream influence occur in meandering rivers? Two simple examples may clarify the problem we wish to investigate. Assume that a meandering river flows in a valley bounded downstream by a canyon: the stream is obviously forced to flow through the canyon, hence a constraint on the position and direction of the channel axis is forced at some downstream

[1]Dipartimento di Ingegneria Idraulica, Marittima Ambientale e Geotecnica, Università di Padova, Padua, Italy.
[2]Dipartimento di Ingegneria Ambientale, Università di Genova, Genoa, Italy.

0148-0227/06/2005JF000416$09.00

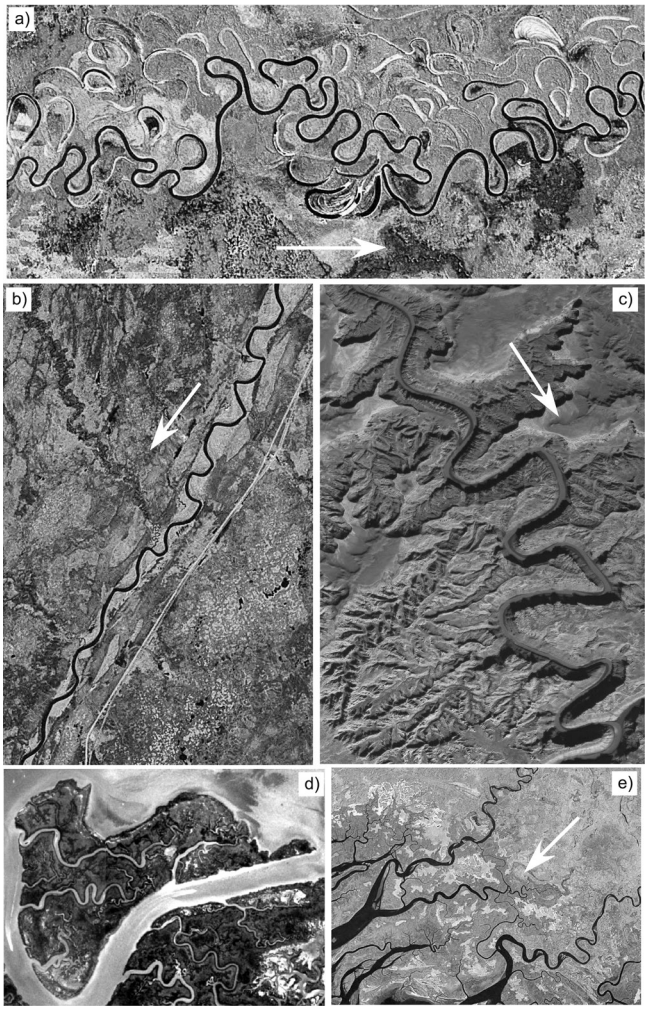

Figure 1. Examples of meandering patterns: (a) meanders wandering through a flat valley (western Canada): several abandoned loops (oxbow lakes) are shown, multiple loops are present, and upstream and downstream skewing coexist; (b) meanders constrained within a narrow valley (western Canada); (c) meanders carved in a rocky environment (Utah, United States); (d) tidal meanders cut through the salt marshes of the Venice lagoon (Italy), and (e) along the Tanzania coast. The arrows indicate either the flow (Figures 1a, 1b, and 1c) or the seaward direction (Figure 1e). The images have been obtained by Landsat mosaic images (Figures 1a, 1b, 1c, and 1e, https://zulu.ssc.nasa.gov/mrsid/mrsid.pl) and aerial lidar images (Figure 1d).

cross section: how will this constraint be felt upstream? As a second example, consider a meandering river flowing into the sea: how will the downstream constraint on the elevation, forcing the free surface at the outlet, influence the planform development of the river?

[5] The issue of upstream and downstream influence in the planform evolution of meandering rivers is related to a problem discussed by *Zolezzi and Seminara* [2001]: how does the presence of a bend affect bed topography in the downstream and upstream reaches? *Struiksma et al.* [1985] performed enlightening experiments in erodible channels with constant curvature and nonerodible banks, connected both upstream and downstream with straight channel reaches. They invariably detected downstream influence, i.e., a stationary bar, with spatial fluctuations of bed topography along both the inner and outer banks, developed downstream of the entrance of the curved reach, leading eventually to the formation of a point bar in equilibrium. Also, the bed deformation at the exit section of the bend led to a similar damped stationary bar in the downstream reach.

[6] *Zolezzi and Seminara* [2001] and *Zolezzi et al.* [2005] extended the above ideas, showing theoretically and experimentally that two distinct scenarios of morphodynamic influence may arise, depending on the values attained by the relevant physical parameters. In particular, for fairly wide channels, upstream influence may also occur: in this case, the presence of the bend generates damped spatial fluctuations of bed topography along both the inner and outer banks in the upstream reach.

[7] A number of consequences for the mechanics of meander development arise from the distinction between upstream and downstream influence: some of them have been pointed out by *Seminara et al.* [2001]. Here, we wish to develop further the above ideas, setting the problem on a firmer basis in the light of the recognition that meander development is the expression of a planform instability. The rational framework for meander formation proposed in the fundamental contribution of *Ikeda et al.* [1981] and widely followed since, is essentially based on the following scheme. Assume that a uniform straight channel is in morphodynamic equilibrium. Perturbations of channel alignment in the form of sequences of small amplitude meanders then induce the formation of forced bars, which drive erosion at the outer banks and deposition at the inner banks, leading to meander growth and migration. Having recognized that meanders develop as a result of an instability process, we may then employ a classical approach of stability theory to ascertain the nature of this instability. What do we mean by "nature of an instability"? Technically an instability is described as convective if an initial, nonpersistent, small perturbation localized in space is convected away (typically, though not necessarily, in the direction of the main flow) leaving, as time grows, the original pattern unperturbed. An instability may alternatively be absolute: this occurs whenever an initial small localized perturbation spreads both in the upstream and downstream directions as time grows, affecting eventually the whole flow domain. Such a fundamental classification was originally proposed in the field of plasma physics [*Briggs*, 1964; *Bers*, 1975] and later applied in various different contexts including hydrodynamic stability (see the review by *Huerre and Monkewitz* [1990]).

[8] The reader should fully appreciate the fundamental distinction between the two types of instabilities: first, convective instabilities require a persistent perturbation located at some initial cross section of the channel, while absolute instabilities develop even if perturbations are triggered at some initial time and then cease; secondly, a convective instability forced by a persistent perturbation affects the channel in only one direction (either upstream or downstream), while an absolute instability leads to both upstream and downstream influence. The latter feature clarifies how this apparently abstract viewpoint relates to our original question.

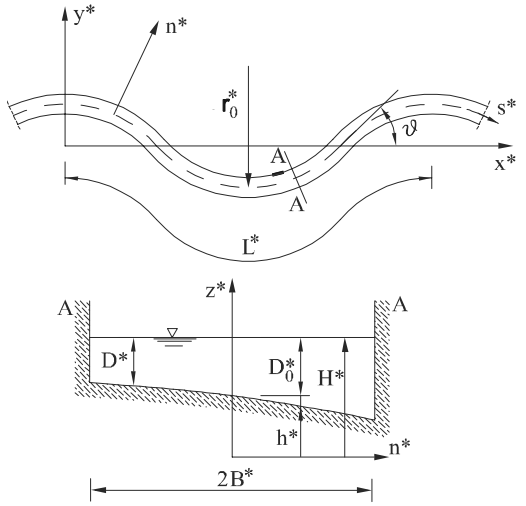

Figure 2. Sketch of a meandering channel and notations.

[9] In section 2, we employ some classical mathematical tools to analyze the nature of bend instability which turns out to be mostly, though not invariably, convective at a linear level: a small perturbation of the channel axis is found to develop into a group of meander waves which grows and migrates. Moreover, an interesting further feature arises: the group velocity of the bend perturbation changes sign; that is, the direction of meander migration shifts from downstream to upstream, as some threshold condition for the relevant physical parameters is crossed. Above this threshold, the morphodynamics is dominantly controlled by conditions imposed downstream (upstream influence). We next investigate numerically (section 3) the role of geometric nonlinearity; that is, we follow the development of large amplitude meander planforms. The numerical simulations confirm that the nature of bend instability does not change in the nonlinear regime. Moreover, we discuss the implications of these results on the morphologic characteristics of meandering rivers, in particular the sense of skewing of meander bends and the direction of meander migration, confirming and extending previous results of *Seminara et al.* [2001]. We also investigate the role played by boundary conditions in numerical simulations of planform evolution, and show that their choice is crucially dependent on the nature of bend instability and on its subresonant or superresonant regime. Finally, section 5 concludes the paper with some suggestions for field investigations prompted by the above theoretical framework, along with some remarks on the limits of the present analysis and the need for further developments.

2. Nature of Bend Instability: Linear Theory

[10] Let us first summarize the problem of planform evolution of meandering channels. An extremely effective framework, stemming from the early work of *Ikeda et al.* [1981], consists of representing the river planform through its channel centerline. Predicting the planform evolution of the river can then be ultimately reduced to the problem of determining the motion of a line lying on a plane, such that each point of the line moves in the normal direction with some lateral migration speed driven by bank erosion. An intrinsic dimensionless formulation of this rule was derived by *Seminara et al.* [1994] and leads to the following nonlinear, integrodifferential planimetric evolution equation:

$$\frac{\partial \theta}{\partial t} - \frac{\partial \theta}{\partial s} \int_0^s \zeta \frac{\partial \theta}{\partial s}\, ds = \frac{\partial \zeta}{\partial s} \tag{1}$$

where $\theta(s, t)$ is the angle that the local tangent to the channel axis forms with a Cartesian axis x^* (Figure 2), s is the longitudinal coordinate, scaled by half the channel width B^*, ζ is the lateral migration speed of the channel, scaled by some reference speed U_0^*, while t is time, scaled by B^*/U_0^*. Note that, hereafter, a star denotes dimensional quantities.

[11] Hence channel deformation is affected by the whole previous history of the process, a feature which emerges from the integrodifferential character of equation (1).

[12] The mathematical formulation of bend instability next requires an erosion law relating the lateral migration speed of the channel ζ to the stream hydrodynamics, which in turn depend on channel curvature. We follow *Ikeda et al.* [1981] and write

$$\zeta = E\left(U|_{n=1} - U|_{n=-1}\right) \tag{2}$$

with U the depth averaged longitudinal velocity, scaled by the reference speed U_0^*, n the lateral coordinate, with origin at the channel axis, scaled by the half channel width, and E a dimensionless long-term erosion coefficient. The above law essentially states that bank erosion is driven by excess flow speed at the outer bank accompanied by a decreased flow speed at the inner bank. Note that pure width variations, arising from the erosion of (or deposition at) both banks, do not produce any lateral migration of the channel centerline: these perturbations, in fact, do not affect the relationship (2), which then preserves channel width throughout the meander evolution process. Also note that equation (2) is not a representation of the actual mechanical process which drives bank erosion at the temporal scale of flood propagation: indeed, bank collapse is due to a complicated mechanism depending on several factors, including the intensity of scour at the bank toe, the cohesive properties of the banks, and the process of drainage induced by the wetting and drying of banks as stage varies. Moreover, the rate controlling process is the ability of the stream to remove sediments accumulated at the bank foot [*Darby*, 1998; *Darby et al.*, 2002]. This notwithstanding, equation (2) proves quite successful as an integrated descriptor of the long-term evolution of the erosion process: it essentially locates the region of the outer bank where erosion occurs and provides a continuous description of an actually intermittent process.

[13] In order to complete the mathematical formulation we finally need a hydrodynamic model of flow in sinuous channels with cohesionless bed and an arbitrary distribution of channel curvature. The availability of such a model allows us to determine the quantity $(U|_{n=1} - U|_{n=-1})$ appearing in equation (2) as a function of channel curvature ($\approx -\theta_{,s}$). Substituting the latter into equation (1), the problem for the unknown function $\theta(s, t)$ is closed and just requires to impose appropriate boundary and initial con-

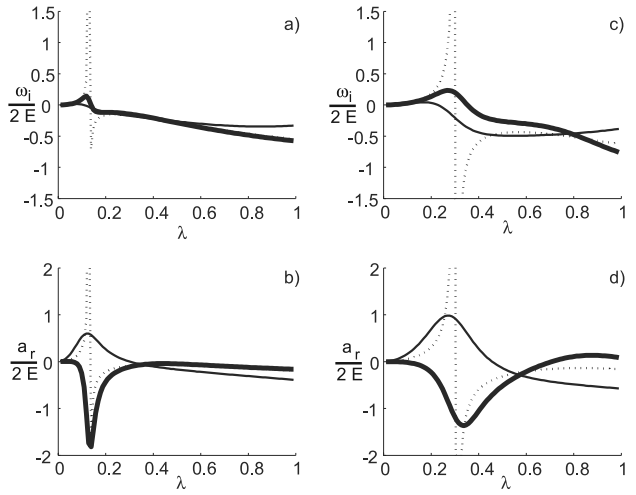

Figure 3. Dependence of temporal growth rate ω_i and migration speed a_r on real meander wave number. Three lateral Fourier modes have been used to describe the flow field; indeed, considering further modes does not change the results quantitatively. (a, b) Plots referring to plane bed conditions ($\tau^* = 0.1$, $d = 0.01$) and (c, d) plots obtained by assuming a dune-covered bed ($\tau^* = 0.3$, $d = 0.005$). Thin lines denote subresonant conditions (Figures 3a and 3b, $\beta = 10$; Figures 3c and 3d, $\beta = 5$); thick lines denote superresonant conditions (Figures 3a and 3b, $\beta = 25$; Figures 3c and 3d, $\beta = 15$); dotted lines denote resonant conditions (Figures 3a and 3b, $\beta_r = 20$; Figures 3c and 3d, $\beta_r = 10$).

ditions. A number of hydrodynamic models have been proposed in the literature. Here, we refer to two linear models which predict various important mechanisms operating in bend instability. Both models have been derived under the assumptions of steady flow conditions, bed load dominated sediment transport, and do not account for the possible coexistence of free migrating and forced steady bars. The first model was proposed by *Ikeda et al.* [1981] for sequences of sine generated meanders. The second model was proposed for sequences of sine generated meanders by *Blondeaux and Seminara* [1985] and later extended to rivers with arbitrary (though slowly varying) distributions of channel curvature by *Zolezzi and Seminara* [2001]. The major difference between the two models is the full coupling between hydrodynamics and sediment transport present in the second model, where the shape of bed topography is not assumed a priori.

[14] We now perform a planimetric stability analysis. The basic state of the channel is taken to be the straight configuration, defined by the simple relationship $\theta = 0$. We then investigate the conditions for a small perturbation of this basic state to grow. A classical normal mode approach is in this case of particular interest, as it is equivalent to investigating perturbed states consisting of a sequence of so-called sine generated meanders [*Langbein and Leopold*, 1964] which are characterized by a sinusoidal distribution of channel curvature. Mathematically, our perturbed states can be expressed as

$$\theta = \theta_1 \exp i(\lambda s - \omega t) \tag{3}$$

where θ_1 is the small initial amplitude of the perturbation, λ is the intrinsic meander wave number, scaled by $1/B^*$, ω is the angular frequency, scaled by U_0^*/B_0^*, and i is the imaginary unit. The temporal growth rate of the disturbances coincides with the imaginary part, ω_i, of the angular frequency while the dimensionless complex phase and group velocities are given by $a = \omega/\lambda$ and $\partial\omega/\partial\lambda$, respectively.

[15] Employing the linearized form of the bend evolution equation (1), the erosion rule (2), and some hydrodynamic model, one eventually derives a dispersion relationship for bend instability, that is, a relationship between the complex quantity ω and the meander wave number λ. The form of this relationship obtained by *Seminara et al.* [2001] is

$$\omega = 2E \sum_{m=0}^{\infty} (-1)^{m+1} A_m \lambda \left[\sum_{j=1}^{5} \rho_j (i\lambda)^j \right] \Bigg/ \left[\sum_{j=0}^{4} \sigma_i (j\lambda)^j \right] \tag{4}$$

where A_m is a coefficient quantifying the decaying contributions of higher lateral Fourier modes of the solution, while ρ_j and σ_j are functions of the relevant dimensionless parameters, namely, the aspect ratio β (half width to depth), the Shields parameter τ_* (a dimensionless measure of bottom stress) and the average friction coefficient C_{f0}. With the notations of Figure 2, β and τ_* are given by

$$\beta = \frac{B^*}{D_0^*}, \qquad \tau_* = \frac{C_{f0} U_0^{*2}}{\Delta D_0^* d} \tag{5}$$

where Δ is the relative submerged density of sediment particles and d is the sediment diameter, taken to be uniform and scaled by the average flow depth D_0^*. From equation (4) one easily finds relationships for meander growth rate (ω_i) and migration speed a_r as functions of meander wave number λ, for given values of the aspect ratio β and of the Shields parameter τ_*.

[16] In Figure 3 we have plotted the dispersion relationship (4) for realistic values of the relevant parameters. Various features arise.

[17] 1. Small amplitude, sine generated meanders amplify for values of the meander wave number λ smaller than some threshold value, while shorter meanders decay. Moreover, a peak in the growth rate is observed at a value of the dimensionless wave number ranging from about 0.1 to 0.3 (corresponding to wavelengths of about 30 and 10 channel widths, respectively), as shown in Figures 3a and 3c.

[18] 2. The peak growth rate tends to infinity for specific values of the intrinsic meander wave number, λ_r, and of the aspect ratio, β_r, depending on the intensity of sediment transport (τ_*) and friction (C_{f0}). The functions $\lambda_r(\tau_*)$ and $\beta_r(\tau_*)$ are plotted by *Seminara and Tubino* [1992]. Peaking is associated with the occurrence of resonance [*Blondeaux and Seminara*, 1985]: the response of the channel (which would not develop spontaneously, but is excited at resonance) is a natural nonmigrating perturbation of the cohesionless bed of a straight channel. The bed pattern associated with this perturbation consists of stationary sediment waves, arranged in periodic sequences of riffles and pools in alternate fashion as in the analogue bar pool pattern observed in meandering channels.

[19] 3. The meandering pattern migrates while amplifying. This feature can be shown to arise from the occurrence

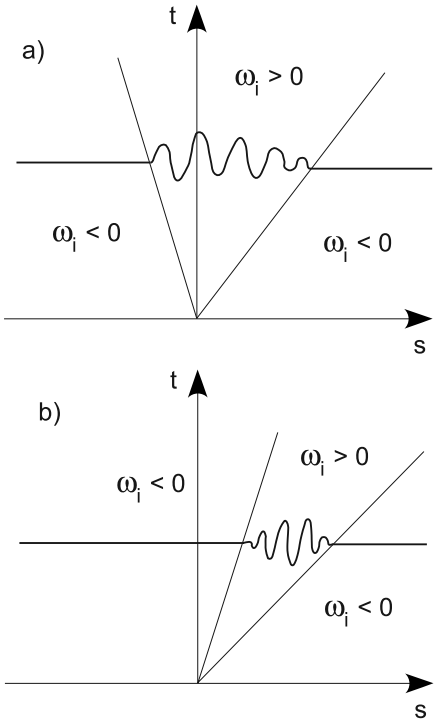

Figure 4. Sketch of a typical impulse response: (a) absolute instability and (b) convective instability.

of a phase lag between peak erosion and peak curvature. Interestingly enough, the migration speed changes sign as the resonance conditions are crossed (3b,d). This feature is related to a well known property of linear resonators [*Kevorkian and Cole*, 1981, p. 141]. In the meander case, crossing resonance (i.e., when the meander wave number λ increases beyond λ_r for given aspect ratio β or, vice versa, when the aspect ratio β increases beyond β_r for given meander wave number λ) causes a shift upstream/downstream of the bend apex of the section characterized by the maximum flow velocity. This has been experimentally confirmed by *Colombini et al.* [1992], as well as by *Garcia and Nino* [1995]. As a result, subresonant (superresonant) trains of periodic meanders migrate downstream (upstream) as found by *Seminara et al.* [2001]. Note, that the dispersion relationship arising from the use of the model of *Ikeda et al.* [1981] is unable to predict resonance and the different behavior of subresonant versus superresonant meanders.

[20] The above results appear to provide a consistent picture of the linear properties of bend instability, although upstream migration of isolated river bends is only occasionally observed and, as discussed in the last section, a systematic field validation of the above picture is as yet unavailable. Let us attempt to extend the above picture by investigating whether the nature of bend instability is convective or absolute. From a mathematical point of view, the nature of the instability can be determined by studying the impulse response of the system, i.e., the behavior of the planform shape arising in response to a spatially localized perturbation imposed at some cross section at the initial time. Such a response has typically the form of a wave packet in the (s,t) plane (see Figure 4). Details of the approach are found in work by *Huerre and Monkewitz* [1990] and *Drazin and Reid* [1981], to which we refer the interested reader. Below, we summarize it briefly. Readers who are not interested in fully appreciating the mathematical basis of our results may proceed directly to the next section.

[21] Using the method of steepest descent [*Morse and Feshbach*, 1953] it can be shown that, in order to distinguish between convective and absolute instability, we must examine the long-term behavior of the impulse response along the ray $s/t = 0$ at a fixed spatial location. In order to see how this goal is achieved, let us recall a few definitions, strictly related to the properties of multiple-valued complex functions. Spatial branches of the dispersion relationship are obtained by solving the dispersion relationship in terms of

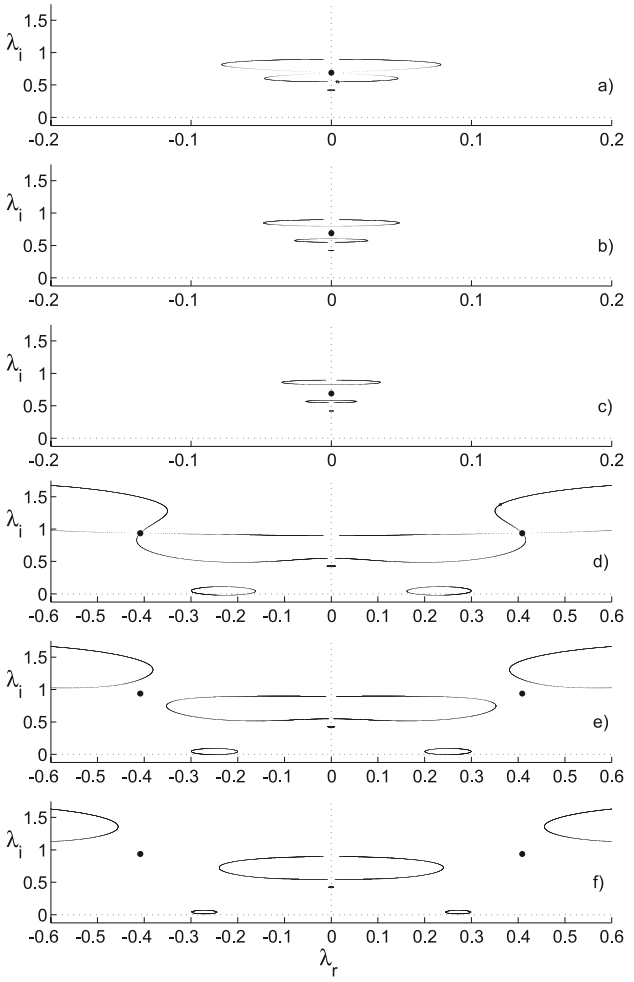

Figure 5. Behavior of the spatial branches of the dispersion relationship, obtained by solving equation (4) in terms of the complex wave number λ as a function of ω_r and for a fixed value of ω_i, plotted in the λ plane for $M = 3$, $\beta = 8$, $\tau_* = 0.3$, $d = 0.005$, dune-covered bed conditions, and (a, d) $\omega_i = [\omega_i]_{\lambda_{0j}}$, (b, e) $\omega_i = 1.5\ [\omega_i]_{\lambda_{0j}}$, and (c, f) $\omega_i = 2\ [\omega_i]_{\lambda_{0j}}$ ($j = 0, 1, 2$). Three branch point singularities (i.e., the points denoted by a solid circle where two or more spatial branches merge) are found: one purely imaginary, λ_{00}, and two complex, λ_{01} and λ_{02}. The spatial branches are always contained in the half plane $\lambda_i > 0$, thus pointing at a convective instability.

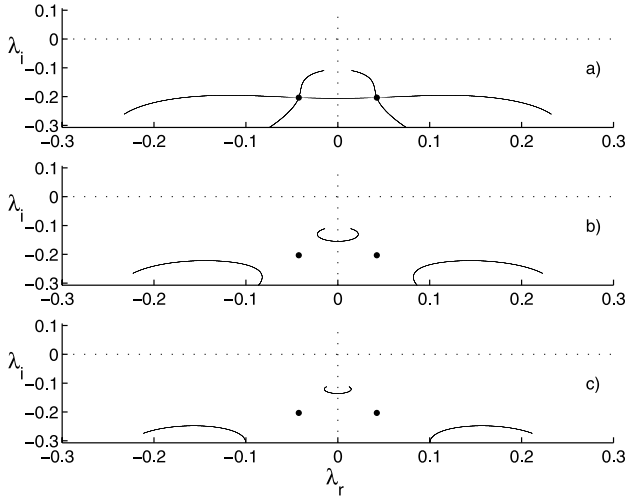

Figure 6. Behavior of the spatial branches of the dispersion relationship, obtained by solving equation (4) in terms of the complex wave number λ as a function of ω_r and for a fixed value of ω_i, plotted in the λ plane for $M = 3$, $\beta = 25$, $\tau_* = 0.7$, $d = 0.005$, dune-covered bed conditions, and (a) $\omega_i = [\omega_i]_{\lambda_{0j}}$, (b) $\omega_i = 1.2\,[\omega_i]_{\lambda_{0j}}$, and (c) $\omega_i = 1.5\,[\omega_i]_{\lambda_{0j}}$ ($j = 1, 2$). The two complex branch point singularities λ_{01} and λ_{02} (i.e., the points where two or more spatial branches merge) are denoted by a solid circle. The spatial branches are always contained in the half plane $\lambda_i < 0$, thus pointing at a convective instability.

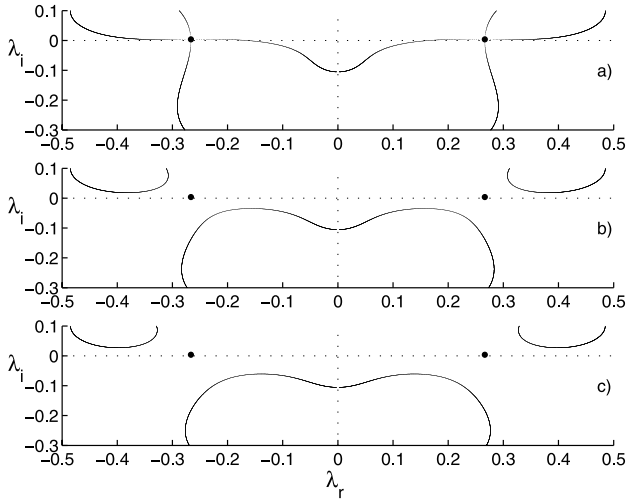

Figure 7. The behavior of the spatial branches of the dispersion relationship, namely, the lines obtained by solving equation (4) in terms of the complex wave number λ as a function of ω_r and for a fixed value of ω_i, plotted in the λ plane for $M = 3$, $\beta = 25$, $\tau_* = 0.7$, $d = 0.005$, dune-covered bed conditions, and (a) $\omega_i = [\omega_i]_{\lambda_{0j}}$, (b) $\omega_i = 2\,[\omega_i]_{\lambda_{0j}}$, and (c) $\omega_i = 5\,[\omega_i]_{\lambda_{0j}}$ ($j = 1, 2$). The two complex branch point singularities λ_{01} and λ_{02} (i.e., the points where two or more spatial branches merge) are marked by a solid circle. The spatial branches are not always contained in the half plane $\lambda_i < 0$, thus pointing at an absolute instability.

the complex wave number λ as a function of ω_r and for a fixed value of ω_i. Branch point singularities are points (ω_0, λ_0) of the parameter space where two or more spatial branches of the dispersion relationship merge: at such points the group velocity $[\partial\omega/\partial\lambda]_{\omega_0,\lambda_0}$ vanishes.

[22] It can then be demonstrated that the long-term behavior of the group of meander waves arising in response to an isolated perturbation of the initially straight configuration of the channel axis is determined by analyzing the branch point singularities of the dispersion relationship for complex frequencies ω and wave numbers λ. In particular, a necessary condition for the instability to be absolute is that the perturbation growth rate $[\omega_i]_{\lambda_0}$ at the branch point must be positive. This condition is also sufficient provided at least two of the spatial branches of the dispersion relationship lie in distinct half λ planes for sufficiently large values of ω_i.

[23] The analysis of the spatial branches of equation (4) in the λ plane as we move from every branch point suggests the existence of two typical scenarios. The first scenario, illustrated in Figure 5, is attained for singularities arising when β is low enough: under such conditions, at a linear level, bend instability appears to be invariably convective. Indeed, the spatial branches emerging from the various branch points characterized by $[\omega_i]_{\lambda_0} > 0$ always lie in the same half λ plane as ω_i is progressively increased starting from the value $[\omega_i]_{\lambda_0}$.

[24] The second scenario emerges for high values of β and is characterized by the existence of four complex branch points. Two of them arise also if only one Fourier mode is included ($M = 1$) and, as shown in Figure 6, point at a convective character of the instability: in fact, they are characterized by spatial branches keeping within the same half λ plane as ω_i is progressively increased. In contrast, the spatial branches emerging from the remaining two singularities (which arise only provided $M > 1$) are found (Figure 7)

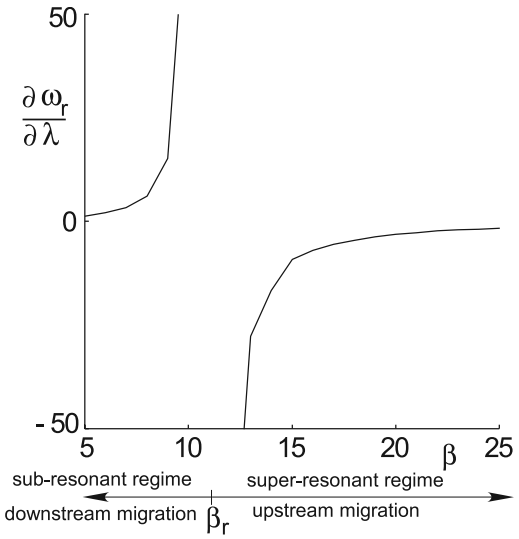

Figure 8. Group velocity $\partial\omega_r/\partial\lambda$ of the meander train developed as a linear response to a localized bend perturbation plotted versus the aspect ratio β for given values of the relevant physical parameters ($\tau_* = 0.2$, $d_s = 0.001$; dune-covered bed).

Figure 9. Typical example of fattened and skewed meander loops (Okavango Delta, Botswana).

to lie in distinct half λ planes. The above results indicate that, at a linear level, bend instability is generally convective, but a transition to absolute instability occurs for large values of β, dune-covered beds and large values of τ_*. Note that, under plane bed conditions a similar behavior is observed, but for unrealistically high values of β.

[25] One final interesting feature of bend instability emerges from the linear analysis: the group velocity $[\partial\omega_r/\partial\lambda]_{\lambda_{max}}$ (with λ_{max} the wave number characterized by maximum growth rate) changes sign as resonance is crossed. This behavior, illustrated in Figure 8, implies that under superresonant conditions the meander pattern propagates upstream. In the next section we simulate numerically the nonlinear planimetric development of a sequence of meanders in order to ascertain whether this linear picture persists as meanders evolve from incipient formation to cut off.

3. Nature of Bend Instability: Geometrically Nonlinear Theory

[26] Field evidence, analytical and numerical studies have clarified that the shape of mature meanders is established through a number of mechanisms experienced throughout the evolution process. Some of these mechanisms, namely, nonlinear interactions among the various harmonics associated with geometric nonlinearity of the meander pattern, abrupt channel shortening via neck and chute cutoffs, spatial heterogeneity of bank erodibility, and grain sorting have received attention in the several models proposed in the recent past [e.g., *Howard and Knutson*, 1984, *Howard*, 1992, 1996; *Parker et al.*, 1982, 1983; *Parker and Andrews*, 1986; *Crosato*, 1990; *Sun et al.*, 1996, 2001; *Seminara et al.*, 1994, 2001].

[27] A number of field observations have been interpreted through the latter studies. In particular, it may be useful to recall the following results. Using a time-dependent nonlinear expansion, based on the idea that the meander wave number may vary in time, *Seminara et al.* [2001] demonstrated that a periodic sequence of large amplitude meanders attains the fattened and skewed shape typically observed in nature (see Figure 9), and described by the classical *Kinoshita* [1961] curve:

$$\frac{d\theta}{ds} = -\nu_0[\cos(\lambda s) - c_F \cos(3\lambda s) - c_S \sin(3\lambda s)] \qquad (6)$$

where ν_0 is the curvature ratio, defined as the ratio of half channel width to some characteristic value of the radius of curvature, say its minimum value in the meandering reach, while c_F and c_S are the fattening and skewing coefficients. This curve, rather than a simple empirical correlation, turns out to be a rational approximation of the exact periodic solution of the planimetric evolution equation (1).

[28] Moreover, the distinction between subresonant and superresonant channels leads to a rich picture. The classical behavior of meanders, shown in Figure 10, is characterized by upstream skewing and downstream migration. In contrast, downstream skewing and upstream migration are obtained under superresonant conditions; clear examples of downstream skewing are displayed in Figure 11. Also, the theoretical analysis of *Seminara et al.* [2001] reproduced the well known monotonic reduction of the migration speed of natural meanders, which tends to vanish prior to cutoff [*Nanson and Hickin*, 1983], as well as the initial increase of the lateral migration of meander trains followed by a monotonic decrease. In any case, meanders of permanent form (i.e., perturbations which display neither growth nor decay) are not possible [*Parker et al.*, 1983; *Parker and Andrews*, 1986; *Seminara et al.*, 2001]. In the absence of geological constraints (like valley confinement), meanders evolve continuously until cutoff processes locally straighten the channel axis. Finally, numerical simulations of the planform evolution, carried out starting from a straight, slightly and randomly perturbed initial configura-

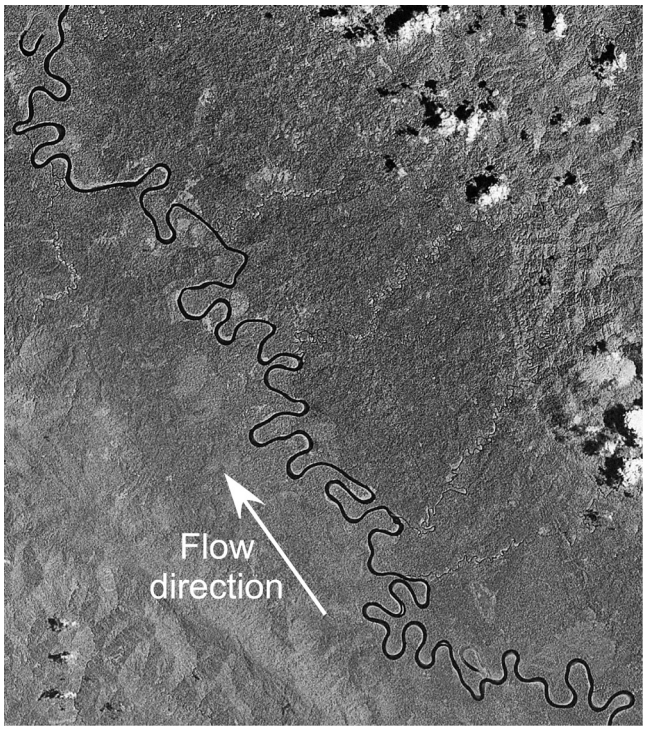

Figure 10. Example of the planimetric pattern of an upstream skewed meandering river located in the northern part of Papua New Guinea. The images have been obtained from Landsat mosaic images (https://zulu.ssc.nasa.gov/mrsid/mrsid.pl). The arrow indicates flow direction.

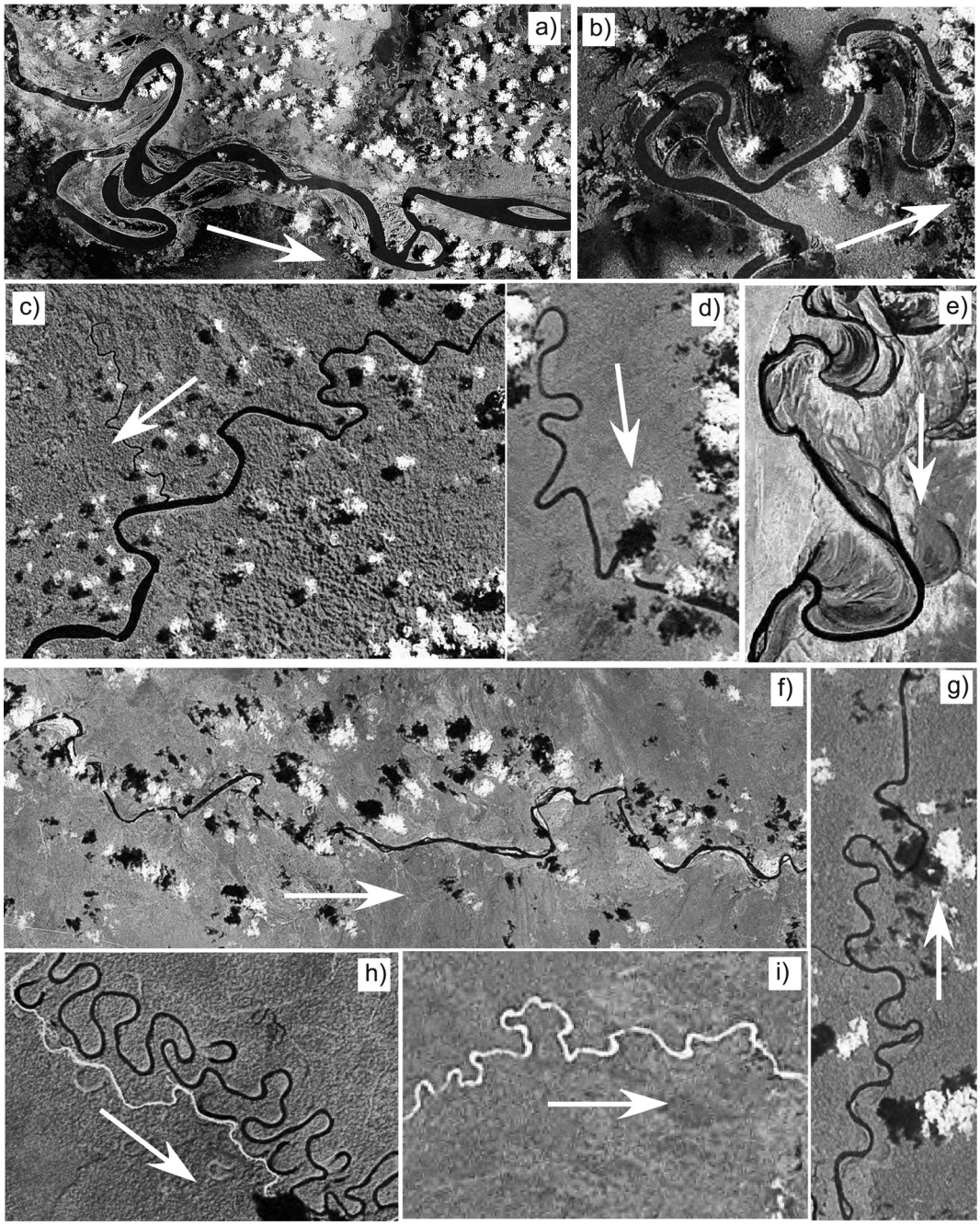

Figure 11. Examples of the planimetric pattern of meandering rivers showing the presence of downstream skewed meandering loops. The rivers are located in (a, b, c) the southern part of Papua New Guinea (in particular, Figures 11a and 11b refer to some reaches of lower and middle Fly River), (d, h, g) the northeastern coast of Papua New Guinea, (e) Namibia, (f) Kenya, and (i) Tanzania. The images have been obtained from Landsat mosaic images (https://zulu.ssc.nasa.gov/mrsid/mrsid.pl). The arrows indicate flow direction.

tion, suggest that the development of compound loops, where upstream and downstream skewed bends coexist, can occur prior to neck cutoff when rivers are brought close to the resonance state [*Sun et al.*, 2001] or evolve much faster under superresonant conditions [*Seminara et al.*, 2001]. A number of compound loops can easily be detected in Figure 10.

[29] One of the major problems left unexplored in the above simulations was the role of boundary conditions: this is a delicate issue which is also of conceptual relevance. In fact, as it will appear from the numerical simulations described below, the nature of boundary conditions appropriate to any given configuration is strictly related to the direction in which morphodynamic influence

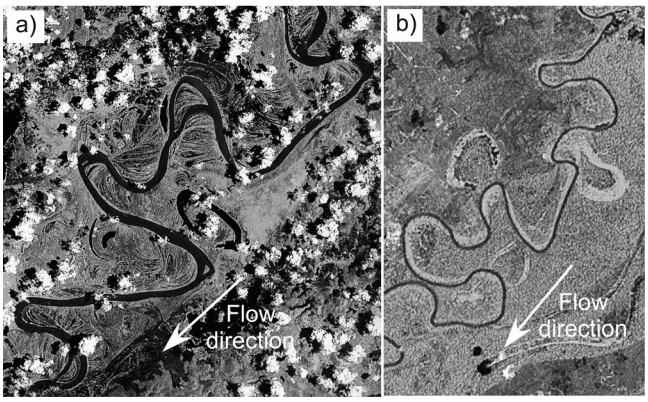

Figure 12. Examples of two planimetric patterns showing some examples of (a) chute and (b) neck cutoffs leading, in both cases, to the formation of oxbow lakes. The images refer to two rivers located in southern (Strickland River) (Figure 12a) and the northern part of Papua New Guinea (Figure 12b) and have been obtained from Landsat mosaic images (https://zulu.ssc.nasa.gov/mrsid/mrsid.pl).

is propagated. We are then led to reconsider the question of the nature of bend instability in a geometrically nonlinear context.

3.1. Description of the Numerical Model

[30] We start from an initial straight planimetric configuration, slightly and randomly perturbed. The channel axis is discretized through a sequence of equally spaced nodes $P_i = (x_i, y_i)$. The very slow timescale associated with the planimetric development of the channel is described in terms of the slow temporal variable $\tau = E\,t$. At every time step $\Delta\tau$, the planimetric evolution of the channel axis is calculated by displacing each node orthogonally to the channel centerline by an amount $\hat{\zeta}\Delta\tau$, with the normalized migration velocity $\hat{\zeta} = \zeta/E$ evaluated through equation (2). In our simulations a constant erodibility coefficient was assumed, while the depth averaged values of the longitudinal velocity U at the inner and outer banks were calculated through the analytical solution obtained by *Zolezzi and Seminara* [2001]

$$U = 1 + \nu_0 \sum_{m=0}^{\infty} u_m \sin(2m+1)\pi n/2 \tag{7}$$

where the amplitude of the mth lateral Fourier mode is

$$u_m = \sum_{j=1}^{4} \left[A_m g_{j0} \int_{s_0}^{s} \mathcal{C}(\xi) e^{\lambda_{mj}(s-\xi)} d\xi + c_{mj} e^{\lambda_{mj}(s-s_0)} + A_m g_{j1} \mathcal{C} \right] \tag{8}$$

Here g_{jk} ($j = 1, 4$; $k = 0, 1$) are coefficients depending on the relevant physical parameters (β, C_{f0}, and τ_*), while λ_{mj} ($m = 0, \infty$; $j = 1, 4$) are characteristic exponents for the mth mode, and c_{mj} are integration constants to be specified on the basis of the boundary conditions at the channel ends. Finally, $\mathcal{C}$ is the local value of the dimensionless channel curvature determined from the geometrical relationship

$$\nu_0 \mathcal{C}(s) = -\frac{d\theta}{ds} \tag{9}$$

where the curvature ratio ν_0 is defined as the ratio of half channel width to some characteristic value of the radius of curvature, say its minimum value in the meandering reach. In particular, the value attained by θ at each node was determined by averaging back and forth, as described by *Seminara et al.* [2001]. Central differences were used to calculate the s derivatives of θ, except at the upstream and downstream boundaries, where forward and backward differences were employed, respectively. The convolution integrals in equation (8) account for either upstream or downstream propagating influence, depending on the sign of the real part of the characteristic exponents λ_{mj}. Quadratures were performed using Simpson's rule and taking advantage of the fact that the functions to be integrated decay exponentially. The latter feature, in fact, allows one to truncate the integration when the function to be integrated is smaller than a given tolerance (say 0.0001), with a significant reduction of the computational effort. If the tolerance is achieved before or just at the fifth computational node, the convolution integral is solved analytically, by assuming that the curvature varies linearly between two consecutive nodes.

[31] It is worthwhile to note that spatial derivatives of curvature do not appear explicitly in the relationship for u_m. In fact, in the term

$$\sum_{k=1}^{6} \frac{\partial^{(k-1)}\mathcal{C}}{\partial s^{(k-1)}} \sum_{j=1}^{4} g_{jk} \tag{10}$$

reported in the original work of *Zolezzi and Seminara* [2001], the sum $\Sigma_{j=1}^{4} g_{jk}$ turns out to vanish identically for $k > 1$. On the contrary, the derivatives of the curvature may affect the calculation of the four integration constants c_{mj} (for each m mode), depending on the boundary conditions. However, both the case of channel ends which are not subject to any constraint (in which case the constants c_{mj} vanish identically) and the case of periodic boundary conditions (implying that the curvature of the axis and its derivatives coincide at the upstream and downstream ends of the channel) do not involve the numerically delicate calculation of derivatives of curvature.

[32] In order to improve the accuracy and efficiency of computation, a time marching predictor-corrector method [*Crosato*, 1990] was used. The forward time step was performed using for each node the normalized migration rate obtained by averaging its values at the previous and present time steps. The step size $\Delta\tau$ was controlled by requiring that $\Delta\tau \leq \epsilon \Delta s/(U_{n=1} - U_{n=-1})_{\max}$, where the choice of the value of the parameter ϵ (= 0.1), defining the threshold between stable and unstable computations, was made through suitable simulation tests. As the channel migrates, the distance Δs between individual nodes may increase or decrease. A standard cubic spline interpolation was used to remesh the points uniformly after each time

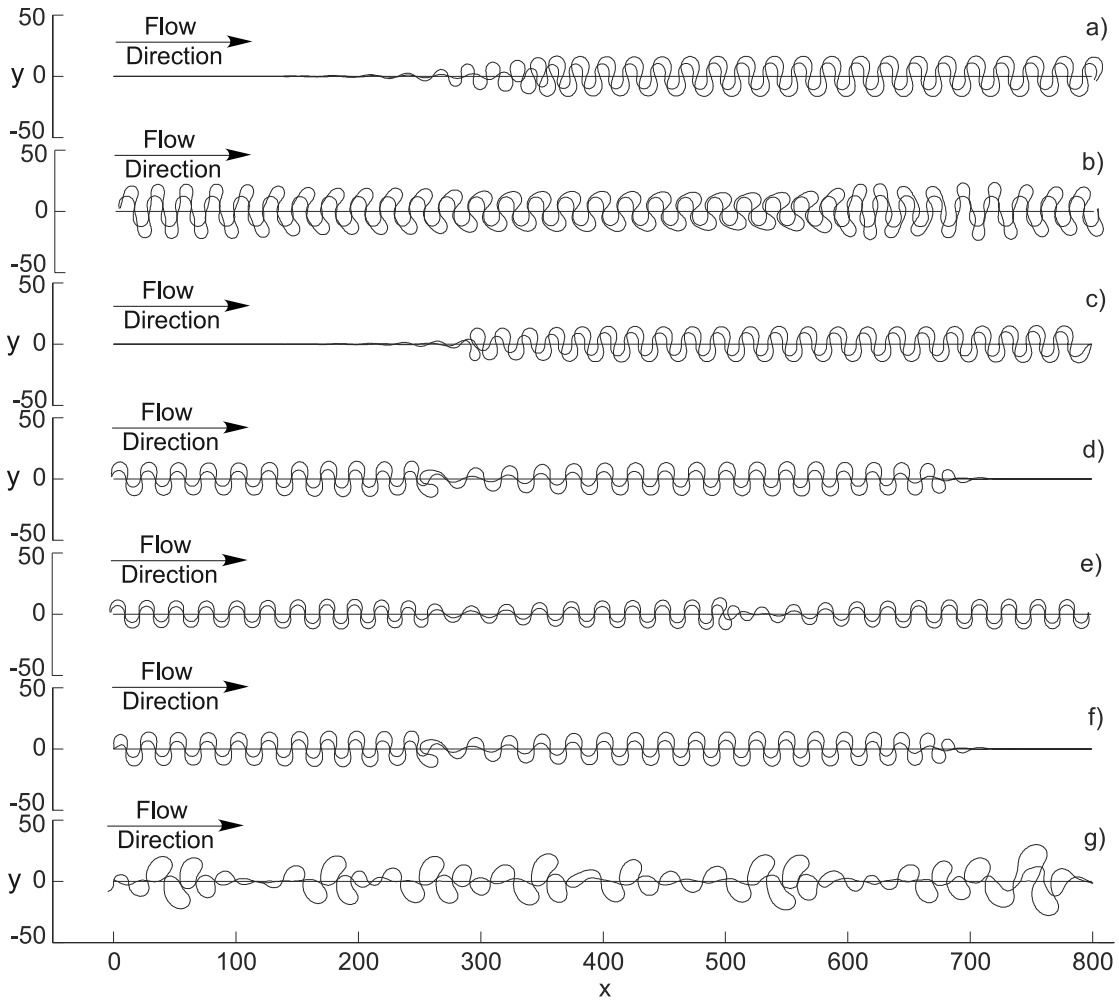

Figure 13. Examples of the planimetric response of an initially straight channel to small random perturbations. All the simulations were carried out setting $E = 10^{-8}$ and assuming a dune-covered bed. Each plot shows the initial channel axis, a configuration at an intermediate time, and the planform pattern at incipient neck cutoff. The following boundary conditions were adopted: (a, d, g) no constraints at both the channel ends, (b, e) periodic boundary conditions, (c) no constraint at the upstream end and downstream channel reach forced to merge into a straight nonerodible canyon, and (f) no constraints at the downstream end and upstream end forced to originate from a nonerodible straight canyon. Runs a, b, and c are characterized by subresonant conditions ($\beta = 9$, $\tau_* = 0.3$, $d_s = 0.005$) and show a convective instability: Wave groups migrate downstream, leaving the upstream reach unperturbed. Runs d, e, and f are characterized by superresonant conditions ($\beta = 13$, $\tau_* = 0.3$, $d_s = 0.005$): Wave groups migrate upstream, leaving the downstream reach unperturbed. Run g is characterized by superresonant conditions ($\beta = 25$, $\tau_* = 0.7$, $d_s = 0.005$), but the instability is absolute: Wave groups migrate upstream but spread over the entire domain.

step. Moreover, new nodes were periodically added to maintain the size of the spatial step in the range $0.8 \sim 0.9$.

[33] The recognition that meanders of permanent form do not develop in the absence of geological constraints, implies that the study of the long-term morphological evolution of a meandering river requires modeling of cutoff processes, which provide local mechanisms to straighten the channel axis, thus limiting the growth of channel sinuosity. Two different types of cutoff are usually recognized in natural channels, chute and neck cutoffs. Chute cutoffs are relatively long flow diversions which occur when a meander loop is bypassed through a new channel which forms across the bar enclosed by the loop (see Figure 12a). This process occurs most frequently in wide channels with large curvature bends, high discharges, poorly cohesive, weakly vegetated banks, and high gradients [*Howard and Knutson*, 1984]. Neck cutoffs occur when the local sinuosity becomes so large that adjacent loops intersect each other, leading to the formation of an abandoned loop (oxbow lake) when sedimentation closes the ends of the former loop (see Figure 12b). In the present simulations we focus our attention only on neck cutoff processes, which characterize the long-term development of highly sinuous meandering rivers. Following *Howard and Knutson* [1984] and *Sun et al.* [1996], the presence of potential neck cutoffs was detected by controlling whether the distance between the

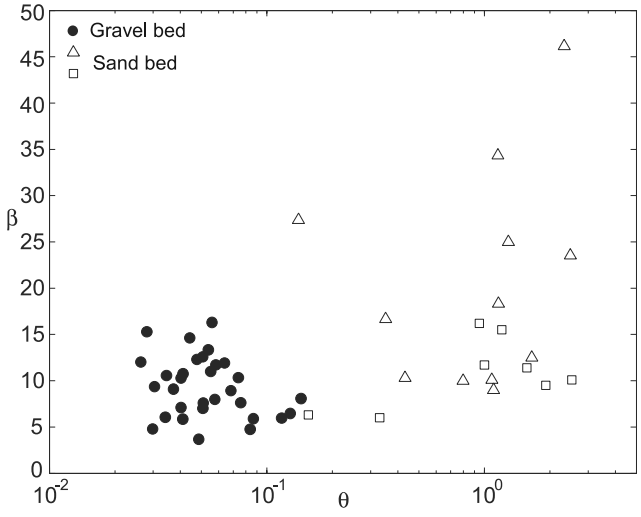

Figure 14. Shields parameter τ_* plotted versus the aspect ratio β for both gravel and sand bed rivers. Sources are as follows: gravel bed river [*Hey and Thorne*, 1986] and sand bed rivers (triangles [*Chitale*, 1970] and squares [*Parker and Johanneson*, 1989]).

*i*th node P_i and a given node P_{i+k} (not immediately upstream or downstream of P_i) approaches some critical distance (say, $2.2B^*$). When such a distance is reached, all the points P_{i+j}, $j = 1, k$, representing the abandoned channel loop, are removed. Furthermore, in order to avoid the presence of physically nonrealistic cusp-like regions with very high curvature at a reconnection, we chose to remove also three nodes upstream of P_i and three points downstream of P_{i+k}. Such a somehow artificial procedure is justified by the fact that, in meandering rivers, the rapid smoothing of sharp bends is a well-known process.

3.2. Numerical Simulations

[34] Some examples of the nonlinear response of the system, starting from a straight channel configuration to which a small random perturbation was superimposed, are shown in Figure 13 referring to morphodynamic conditions similar to those adopted in the linear case (Figures 5–7). The numerical results confirm the picture that emerged from the linear analysis described in the previous section. Bend instability turns out to be generally convective (Figures 13a, 13c, 13d, and 13f), except under superresonant conditions, for dune-covered beds and fairly high values of the Shields stress τ_* (Figure 13g): in the latter conditions an absolute instability is observed. Moreover, the group velocity of the bend perturbation changes sign as the resonant conditions are crossed. This implies that under subresonant (superresonant) conditions, nonpersistent initial perturbations develop into wave groups which amplify and migrate downstream (upstream), leaving the upstream (downstream) reach unperturbed, i.e., recovering the initial straight configuration (Figures 13a, 13c, 13d, and 13f). Note that, in the context of the uncoupled model of *Ikeda et al.* [1981], bend instability is only convective and wave groups can only migrate downstream.

[35] The above findings have interesting implications for the morphology of alluvial rivers and the numerical simulation of their planform evolution. Relatively narrow gravel bed rivers, typically characterized by plane bed conditions and low values of the Shields parameter (Figure 14, but see also G. Parker, 1D Sediment Transport Morphodynamics with Applications to Rivers and Turbidity Currents, 2004, available at http://cee.uiuc.edu/people/parkerg/morphodynamics_e-book.htm, hereinafter referred to as Parker, e-book, 2004) at bankfull stage, are likely subresonant, hence display upstream skewed meander loops (see Figure 10) which migrate downstream. Conversely, wide and shallow gravel bed rivers would be more prone to fall within the superresonant regime, with downstream skewed upstream migrating bends (Figure 11). However, in this case, the high values attained by the aspect ratio favors the growth of multiple bars, i.e., the development of a braided pattern. Interestingly, some recent field observations suggest that the shallow, weakly meandering channels which form in a braided system exhibit morphological features typical of the superresonant regime [*Zanoni et al.*, 2006]. Superresonant conditions are expected to occur also in fairly wide sandy rivers, where the bankfull Shields stress may attain relatively large values (Figure 14, but see also Parker (e-book, 2004)) and the rather common presence of dunes leads to an increased flow resistance. It is important to point out that, as recently found by *Federici and Seminara* [2006], in the presence of suspended load the superresonant regime is associated with values of β smaller than in the case of dominant bed load. A transition from subresonant to superresonant conditions is then to be expected moving toward the seaward portion of alluvial rivers, where the cross sections tend to widen and downstream fining favors transport in suspension. The possible existence of this transition would crucially modify the way the constraint imposed by the sea at the outlet affects the morphodynamics of meandering rivers wandering though coastal plains.

[36] The implications of these results on the numerical simulations of planform evolution are related to the choice of the boundary conditions appropriate to subresonant and superresonant conditions. In particular, imposing periodic boundary conditions, as done by several authors including *Seminara et al.* [2001], is actually not compatible with the convective nature of bend instability [*Deissler*, 1987]. This is clearly detected by comparing the solutions reported in Figures 13a and 13b for the subresonant case, and 13d, 13e for the superresonant case: the free end conditions lead to solutions which are drastically different from those obtained under periodic conditions.

[37] In particular, it is worthwhile to note that, in the simulation portrayed in Figure 13b, the use of periodic boundary conditions gives rise to a planform pattern where compound loops tend to develop prior to neck cutoff and morphological features typical of both the subresonant and superresonant regimes clearly coexist. This result is due to the fact that the value of β (= 9), which is initially slightly subresonant (β_r = 9.5), becomes superresonant as the planform pattern progressively evolves. In fact, channel lengthening usually leads to a decrease of both θ and β. As a consequence of the reduced value of the Shields parameter, also β_r diminishes [see *Seminara and Tubino*, 1992, Figures 3 and 4], the drop being pretty fast for relatively low values of θ. A transition may thus occur from

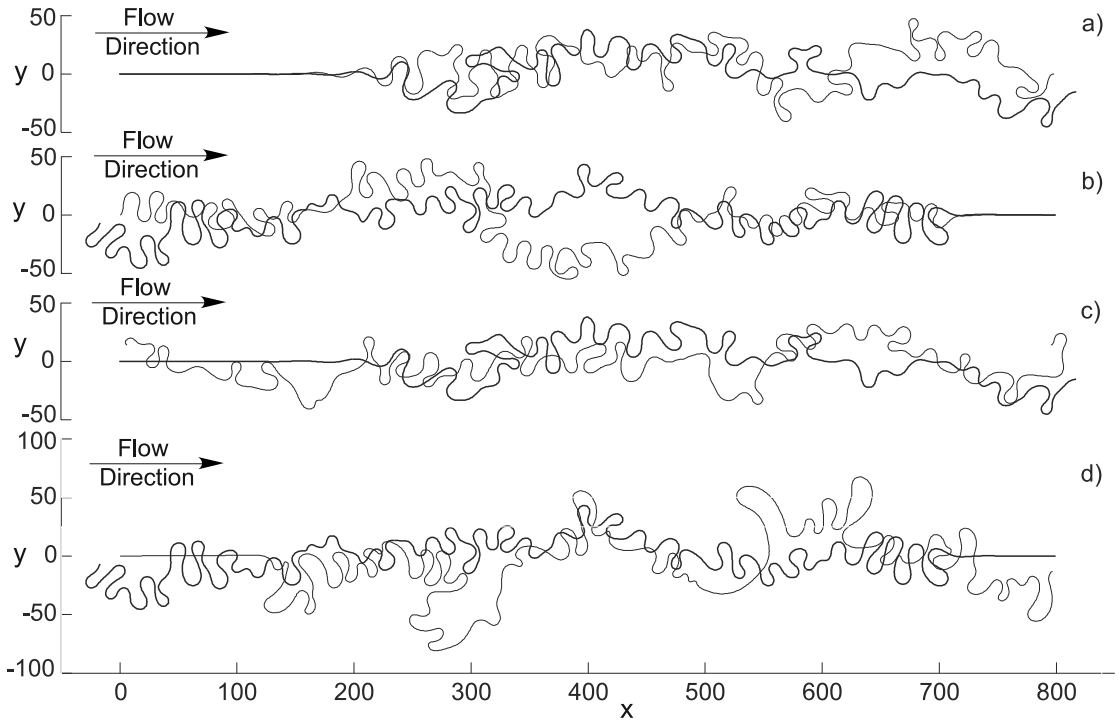

Figure 15. Examples of the long-term response of an initially straight channel to small and random perturbations of channel axis. All the simulations were carried out by setting $E = 10^{-8}$ and assuming a dune-covered bed. The thick lines refer to simulations in which no constraints were imposed at both channel ends. The following boundary conditions were adopted in the simulations depicted with thin lines: (a) no constraint at the upstream end and downstream channel reach forced to merge into a straight nonerodible canyon, (b) no constraints at the downstream end and upstream end forced to originate from a nonerodible straight canyon, and (c) periodic boundary conditions. (d) Comparison between the long-term planform configuration (Figure 15b) obtained imposing no constraints at the channel ends and the one (thin line) resulting from the incomplete model of *Ikeda et al.* [1981] with the modification proposed by *Sun et al.* [1996]. Runs a and c are characterized by subresonant conditions $\beta = 9$, $\tau_* = 0.3$, $d_s = 0.005$, $T = O(10^9)$. Runs b and d are characterized by superresonant conditions $\beta = 13$, $\tau_* = 0.3$, $d_s = 0.005$, $T = O[10^{10}]$.

subresonant to superresonant conditions whenever, as in Figure 13b, β_r decreases faster than β.

[38] Moreover, the issue arises of whether possible geological constraints present in nature may actually be able to propagate their morphodynamic effects throughout the channel. In fact, the nature of bend instability implies that under subresonant conditions the morphodynamic information propagates dominantly downstream. Note that the qualification dominant is necessary as one boundary condition is always available to force some constraint at the downstream end. The scenario is completely reversed under superresonant conditions, for which the morphodynamic information propagates dominantly upstream, as one boundary always applies at the upstream end. Figures 13c and 13f show the consequences of imposing a geological constraint at the downstream (upstream) channel ends, namely, the requirement that the channel must merge into (originate from) a straight canyon. These conditions appear to affect weakly the planform evolution, as the propagation of their effects from the constrained reach is fairly slow because of the fast decay of the spatial mode involved in the expression of this influence.

[39] The simulations reported above, however, have all been stopped before the occurrence of the first neck cutoff. Let us now move to analyze how the boundary conditions affect the evolution of the channel allowed to experience several cutoff events. A few examples of simulations continued after cutoff are shown in Figure 15. It clearly appears that the long-term planform configuration attained by the river is strongly influenced by boundary conditions, which are able to affect the whole reach through the faster mechanism of neck cutoff. In particular, Figures 15a and 15c show the significant differences among the planimetric patterns obtained under subresonant conditions considering, alternatively: (1) no constraints at both the channel ends, (2) no constraint at the upstream end and forcing the downstream channel reach to merge into a straight nonerodible canyon (Figure 15a), and (3) periodic boundary conditions (Figure 15c). Similarly, Figure 15b, referring to superresonant conditions, points out the remarkably different configurations resulting from the application of either no constraints at both the channel ends or no constraints at the downstream end and forcing the upstream channel reach to originate from a straight, nonerodible canyon. Finally, Figure 15d emphasizes

the inability of the incomplete model of *Ikeda et al.* [1981] to simulate superresonant planimetric patterns.

4. Discussion and Concluding Remarks

[40] The analytical and numerical analyses discussed in this paper outline a fairly complete picture of the nature of bend instability. This picture suggests that, for given Shields stress and bottom roughness, a threshold value of the aspect ratio of the channel exists which separates two substantially different regimes, that we have called subresonant and superresonant, following *Blondeaux and Seminara* [1985] and *Zolezzi and Seminara* [2001]. In the former regime, bend instability is invariably convective, the group velocity of meander trains is positive (i.e., downstream migration), and single meanders are typically upstream skewed, according to the usual expectations. In the latter regime, bend instability is generally, though not universally convective, the group velocity of meander trains is negative (i.e., upstream migration), and single meanders are downstream skewed, contrary to the usual expectations. As a consequence, the way the planform evolution is influenced is through morphodynamic information propagating downstream in the former case and upstream in the latter case. These novel results, obtained both in the linear and nonlinear regimes, confirm and extend the previous findings of *Seminara et al.* [2001]; these authors had not investigated the nature of bend instability and raised the problem of morphodynamic influence on the basis of an analysis of the structure of the mathematical solution of the hydrodynamic problem. Moreover, the numerical simulations of *Seminara et al.* [2001] were performed employing periodic boundary conditions, a scheme which we now know to be inappropriate when the instability being modeled has a convective nature. In fact, the second novel feature of the present work is the analysis of the response of the channel pattern to different boundary conditions imposed in numerical simulations of meander development. Under subresonant conditions, when three constraints may be imposed at the upstream end and only one constraint is allowed at the downstream end: the effect of the latter decays quite fast upstream but may be enhanced through the occurrence of neck cutoffs. The opposite occurs in the superresonant case. In general, our simulations show that the planform pattern is crucially dependent on the type of boundary conditions forced at the ends of the channel reach. The above picture has some experimental substantiation. The work of *Zolezzi et al.* [2005] has undoubtedly and conclusively confirmed that upstream influence is observed in the laboratory where, under superresonant conditions, the presence of a bend has been found to give rise to the development of a sequence of bars spatially decaying in the upstream reach. Examples of downstream skewed and upstream migrating meander bends are not unusual (see Figure 11). However, the main goal of the present work is to offer geomorphologists a possibly powerful tool to guide further campaigns of field observations able to provide a conclusive and quantitative substantiation of the whole picture. In fact, from the knowledge of the hydraulic and sedimentologic parameters characterizing a given river reach at bankfull stage (namely, the flow discharge, the average bottom slope and the mean grain size of the bed sediment), the resonant value of the width to depth ratio β_r is easily determined. It is then possible to identify whether the river reach falls in the subresonant or superresonant regime. One may then attempt to ascertain whether meander loops show a tendency to migrate downstream or upstream. Less straightforward is to try to correlate the direction of skewing with the meander regime. In fact, a fully developed meandering pattern is the outcome of a long-term evolution process which is affected by boundary conditions not obviously identified and we have seen that the role of boundary conditions is indeed crucial to determine the response of the system. Moreover, downstream skewing of single bends is often observed in compound loops, which are intrinsically associated with the superresonant character of the channel but may also arise from the occurrence of cutoffs. Field investigations should then be guided by numerical simulations carried out using the set of relevant parameters appropriate to the reach under investigation. This is even more necessary when dealing with mature meander patterns evolving in the stage immediately prior to neck cutoff: under these conditions, the migration speed of meander trains experiences a significant reduction, a further source of difficulty in the interpretation of field observations. Finally, the recognition that a given meandering reach is subresonant or superresonant, i.e., in a specific convective or absolute regime, is also of practical relevance, as it allows to anticipate whether the morphologic effects of engineering works (such as channel dredging, bridge construction, river management or environmental projects) are likely to spread their effects upstream, downstream or throughout the whole reach under investigation.

[41] To conclude, let us recall the simplifying assumptions underlying our analysis. The model is based on a linearized treatment of flow and bed topography, which takes advantage of the fact that, in natural channels, the curvature ratio ν_0 is typically a small parameter (ranging in the interval 0.1–0.2 [*Leopold et al.*, 1964]) and assumes that perturbations originating from deviations of the channel alignment from a straight one are sufficiently small. In other words, the role of flow nonlinearities is ignored. However, the contribution of *Seminara and Solari* [1998] on constant curvature channels, recently extended by *Solari and Seminara* [2005] to channels with arbitrary (yet slowly varying) distribution of channel curvature, suggest that this assumption is reasonable as long as the parameter $\nu_0 \sqrt{\tau_*}/rC_{f0}$ attains values which do not exceed roughly 10. Here r is an empirical parameter falling in the range 0.5–0.6, related to the deviation of sediment trajectories from the direction of the bottom shear stress, a feature arising from the effect of gravity on sloping beds. The model also ignores the possible coexistence of free migrating and forced steady bars. This is unlikely to be a strong limitation, as such a coexistence is known to occur only in the early stage (and possibly in the very late stage) of meander development [*Kinoshita and Miwa*, 1974; *Tubino and Seminara*, 1990]. Sediment transport has been assumed to be bed load dominated, though extensions to the general case would be straightforward. The basic flow has been taken to be steady, an approximation which is justified by our approach which replaces the intermittent character of bank erosion during flood events by an integrated and continuous description of its long-term evolution. This scheme is quite rough and will have to be more deeply coupled with the actual mechanism of bank collapse and the rate limiting

mechanism associated with the removal of sediments stored at the bank toe. The slow spatial variations of the basic flow associated with possible backwater effects have also been ignored along with grain sorting, spatial variations of the flow discharge and the presence of tributaries, spatial variations of erodibility of the floodplain, and vegetation effects. Each of the latter features is likely to play some role in the process which will require attention in the near future.

[42] **Acknowledgments.** The present work has been funded by Cariverona (Progetto MODITE). Partial support has also come from the Ministry of Research and the University of Padua (Progetto di Ateneo Analisi del comportamento morfodinamico di alvei meandriformi in contesti ambientali diversi).

References

Bers, A. (1975), Linear waves and instabilities, in *Physique del Plasmas*, edited by C. DeWitt and J. Peyraud, pp. 117–213, Gordon and Breach, New York.

Blondeaux, P., and G. Seminara (1985), A unified bar-bend theory of river meanders, *J. Fluid Mech.*, *157*, 449–470.

Briggs, R. J. (1964), *Electron-Stream Interaction With Plasmas*, MIT Press, Cambridge, Mass.

Chitale, S. V. (1970), River channel patterns, *J. Hydraul. Div. Am. Soc. Civ. Eng.*, *96*(HY1), 201–221.

Colombini, M., G. Seminara, and M. Tubino (1987), Finite-amplitude alternate bars, *J. Fluid Mech.*, *181*, 213–232.

Colombini, M., M. Tubino, and P. Whiting (1992), Topographic expressions of bars in meandering channels, in *Dynamics of Gravel-Bed Rivers*, edited by P. Billi et al., pp. 457–474, John Wiley, Hoboken, N. J.

Crosato, A. (1990), Simulation of meandering river processes, in *Communication on Hydraulic and Geotechnical Engineering*, *Rep. 903*, Delft Univ. of Technol., Delft, Netherlands.

Darby, S. E. (1998), Modelling width adjustment in straight alluvial channels, *Hydrol. Processes*, *12*, 1299–1321.

Darby, S. E., A. M. Alabyan, and M. Van de Wiel (2002), Numerical simulation of bank erosion and channel migration in meandering rivers, *Water Resour. Res.*, *38*(9), 1163, doi:10.1029/2001WR000602.

Deissler, R. J. (1987), Spatial growing waves, intermittency and convective caos in an open-flow system, *Physica D*, *25*, 233–260.

Drazin, P. G., and W. H. Reid (1981), *Hydrodynamic Stability*, Cambridge Univ. Press, New York.

Einstein, A. (1926), Die Ursache der Meandebildung der Flusslaufe und des sogenannten Baerschen Gesetzes, *Naturwissenschaften*, *12*, 223.

Federici, B., and G. Seminara (2003), On the convective nature of bar instability, *J. Fluid Mech.*, *487*, 125–145.

Federici, B., and G. Seminara (2006), Effect of suspended load on sandbar instability, *Water Resour. Res.*, *42*, W07407, doi:10.1029/2005WR004399.

Fujita, Y., and Y. Muramoto (1985), Study on the process of development of alternate bars, *Bull. Disaster Prev. Res. Inst. Kyoto Univ.*, *35*(3), 55–86.

Garcia, M., and Y. Nino (1995), Dynamics of sediment bars in straight and meandering channels: Experiments on the resonance phenomenon, *J. Hydraul. Res.*, *31*, 739–761.

Hey, R. D., and C. R. Thorne (1986), Stable channels with mobile gravel beds, *J. Hydraul. Eng.*, *112*, 671–689.

Howard, A. (1992), Modelling channel evolution and floodplain morphology, in *Floodplain Processes*, edited by M. G. Anderson, D. E. Walling, and P. D. Bates, pp. 15–62, John Wiley, Hoboken, N. J.

Howard, A. (1996), Modelling channel migration and floodplain development in meandering streams, in *Lowland Flood-Plain Rivers: Geomorphological Perspectives*, edited by P. A. Carling and G. E. Petts, pp. 2–41, John Wiley, Hoboken, N. J.

Howard, A., and T. R. Knutson (1984), Sufficient conditions for river meandering: A simulation approach, *Water Resour. Res.*, *20*(11), 1659–1667.

Huerre, P., and P. A. Monkewitz (1990), Local and global instabilities in spatially developing flows, *Annu. Rev. Fluid Mech.*, *22*, 473–537.

Ikeda, S., and G. Parker (Eds.) (1989), *River Meandering*, *Water Resour. Monogr.*, vol. 12, AGU, Washington, D.C.

Ikeda, S., G. Parker, and K. Sawai (1981), Bend theory of river meanders. part 1. Linear development, *J. Fluid Mech.*, *112*, 363–377.

Imran, J., G. Parker, and C. Pirmez (1999), A nonlinear model of flow in meandering submarine and subaerial channels, *J. Fluid Mech.*, *400*, 231–295.

Johanneson, H., and G. Parker (1989), Linear theory of river meanders, in *River Meandering*, *Water Resour. Monogr. Ser.*, vol. 12, edited by S. Ikeda and G. Parker, pp. 181–214, AGU, Washington, D.C.

Kevorkian, J., and J. D. Cole (1981), *Perturbation Methods in Applied Mathematics*, Springer, New York.

Kinoshita, R. (1961), Investigation of channel deformation on Ishikari river, report, Dep. of Sci. and Technol., Bur. of Resour., Tokyo, Japan.

Kinoshita, R., and H. Miwa (1974), River channel formation which prevents downstream translation of transverse bars (in Japanese), *Shinsabo*, *94*, 12–17.

Langbein, W. B., and L. B. Leopold (1964), Quasi equilibrium states in channel morphology, *Amos. J. Sci.*, *262*, 782–794.

Leopold, L. B., M. G. Wolman, and J. P. Miller (1964), *Fluvial Processes in Geomorphology*, W. H. Freeman, New York.

Mazzocco, G. H. (2005), Studies on Martian landscapes, Ph.D. thesis, 117 pp., Univ. of Padua, Padua, Italy, 31 Dec.

Moore, J. M., A. D. Howard, W. E. Dietrich, and P. M. Schenk (2003), Martian layered fluvial deposit: Implications for Noachian climate scenarios, *Geophys. Res. Lett.*, *30*(24), 2292, doi:10.1029/2003GL019002.

Morse, P. M., and H. Feshbach (1953), *Methods of Theoretical Physics, Part I*, pp. 434–443, McGraw-Hill, New York.

Nanson, G. C., and E. J. Hickin (1983), Channel migration and incision in the Beatton river, *J. Hydraul. Eng.*, *109*, 327–337.

Parker, G., and E. Andrews (1986), On time development of meandes bends, *J. Fluid Mech.*, *162*, 139–156.

Parker, G., and H. Johanneson (1989), Observations on several recent theories of resonance and overdeepening in meandering channels, in *River Meandering*, *Water Resour. Monogr. Ser.*, vol. 12, edited by S. Ikeda and G. Parker, pp. 379–415, AGU, Washington, D. C.

Parker, G., K. Sawai, and S. Ikeda (1982), Bend theory of river meanders. part 2. Nonlinear deformation of finite amplitude bends, *J. Fluid Mech.*, *115*, 303–314.

Parker, G., P. Diplas, and J. Akiyama (1983), Meander bends of high amplitude, *J. Hydraul. Eng.*, *109*, 1323–1337.

Repetto, R., M. Tubino, and G. Zolezzi (1999), Free bars in rivers, *J. Hydraul. Res.*, *37*, 759–775.

Schielen, R., A. Doelman, and H. de Swart (1993), On the nonlinear dynamics of free bars in straight channels, *J. Fluid Mech.*, *252*, 325–356.

Seminara, G. (2005), Meanders, *J. Fluid Mech*, *554*, 271–297.

Seminara, G., and L. Solari (1998), Finite amplitude bed deformations in totally and partially transporting wide channel bends, *Water Resour. Res.*, *34*, 1585–1594.

Seminara, G., and M. Tubino (1989), Alternate bars and meandering: Free, forced and mixed interactions, in *River Meandering*, *Water Resour. Monogr. Ser.*, vol. 12, edited by S. Ikeda and G. Parker, pp. 267–320, AGU, Washington, D. C.

Seminara, G., and M. Tubino (1992), Weakly nonlinear theory of regular meanders, *J. Fluid Mech.*, *244*, 257–288.

Seminara, G., M. Tubino, and D. Zardi (1994), Evoluzione planimetrica dei corsi d'acqua meandriformi dall'incipiente formazione al cutoff, paper presented at XXIV Convegno di Idraulica e Costruzioni Idrauliche, Univ. degli Stud. di Napoli, Naples, Italy, 20–22 Sept.

Seminara, G., G. Zolezzi, M. Tubino, and D. Zardi (2001), Downstream and upstream influence in river meandering. part 2. Planimetric development, *J. Fluid Mech.*, *438*, 213–230.

Solari, L., and G. Seminara (2005), On width variations in river meanders, paper presented at Symposium on River, Coastal, and Estuarine Morphodynamics, Int. Assoc. of Hydraul. Eng., Urbana, Ill., 4–7 Oct.

Struiksma, N., K. W. Olesen, C. Flokstra, and H. De Vriend (1985), Bed deformation in curved alluvial channels, *J. Hydraul. Res.*, *23*, 57–79.

Sun, T., P. Meaking, T. Jossang, and K. Schwarz (1996), A simulation model for meandering rivers, *Water Resour. Res.*, *32*(9), 2937–2954.

Sun, T., P. Meaking, and T. Jossang (2001), A computer model for meandering rivers with multiple bed load sediment sizes: 2. Computer simulations, *Water Resour. Res.*, *37*(8), 2243–2258.

Tubino, M., and G. Seminara (1990), Free-forced interactions in developing meanders and suppression of free bars, *J. Fluid Mech.*, *214*, 131–159.

Zanoni, L., F. Castaman, W. Bertoldi, and G. Zolezzi (2006), Canali meandriformi in alvei intercciati, paper presented at XXX Convegno di Idraulica e Costruzioni Idrauliche, Univ. degli Stud. Roma, Rome.

Zolezzi, G., and G. Seminara (2001), Downstream and upstream influence in river meandering. part 1. General theory and application to overdeepening, *J. Fluid Mech.*, *438*, 183–211.

Zolezzi, G., M. Guala, G. Seminara, and D. Termini (2005), Experimental observations of upstream overdeepening, *J. Fluid Mech.*, *531*, 191–219.

S. Lanzoni, Dipartimento di Ingegneria Idraulica, Marittima Ambientale e Geotecnica, Università di Padova, via Loredan 20, I-35131 Padova, Italy. (lanzo@idra.unipd.it)

G. Seminara, Dipartimento di Ingegneria Ambientale, Università di Genova, via Montallegro 1, I-16145 Genova, Italy. (sem@diam.unige.it)